A 1-kW CW Thin Disc Laser

Christian Stewen, Karsten Contag, Mikhail Larionov, Adolf Giesen, and Helmut Hügel

***Abstract*—The thin disc laser is presented as an optimal laser design for the operation of a quasi-three-level laser active medium in the high power regime with high optical efficiency. Numerical calculations of the laser output power show that operation with an output power up to 1 kW with an optical efficiency of 50% and more is possible at room temperature utilizing 16 absorption passes. Scaling of the output power can be realized by scaling the pumped area using one or more discs. The experimental investigations yield a maximum output power of 647 W at 51% optical efficiency for one crystal and of 1070 W with 48% optical efficiency for four crystals at a temperature of the cooling water of 15 °C.**

***Index Terms*—CW lasers, diode-pumped solid-state lasers, high-power lasers, Yb : YAG.**

I. Introduction

FOR laser operation at high output power with at the same time high optical efficiency and good beam quality, a careful choice of the laser design is required, including the geometry and type of the laser active medium, the pump, and the resonator configuration. With the geometry of a thin disc for the laser active medium, the ratio of cooling surface to pumped volume is increased compared to rod lasers, which is a basic advantage to extract high output power from a small volume. For a good overlap between pump and resonator mode and a high pump power density, a quasi-end pumped geometry is chosen. The operation with good beam quality is possible only if the faces of the disc are cooled, so that the heat flux and the laser beam axis are collinear to each other. As a consequence, thermal lensing effects are dramatically reduced. They stem mainly from a bending of the crystal due to different expansions of its front and back side with additional aberrations resulting from a radial temperature gradient at the edge of the pumped area. Due to the small thickness of the crystal, this configuration leads to a low absorption efficiency since the effective absorbing length is only twice the thickness of the crystal if the unabsorbed pump radiation is reflected at the back side of the crystal. To increase the absorbing length, the unabsorbed pump power is reimaged onto the crystal several times, which is possible if diode lasers are used as pump source. This leads to the design of the thin disc laser [1], as shown in Fig. 1.

The crystal, which is AR coated for the wavelength of the pump and laser radiation at the front side and HR coated for both wavelengths at the back side, is fixed with a layer of indium onto a heat sink, which is typically a copper disc of 1 mm thickness. This disc is mounted on a support and cooled with water from the back side.

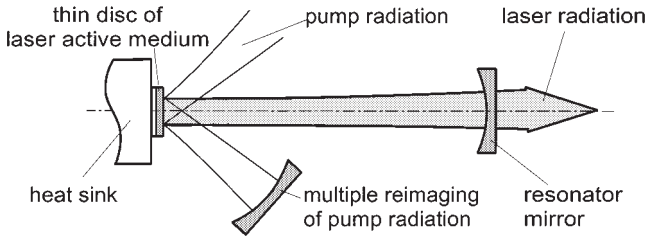

Fig. 1. Principal setup of the thin disc laser.

Repeated passes of the pump radiation through the crystal increase not only the absorption efficiency but also the effective pump power density. Therefore, the thin disc design is suitable for quasi-three-level systems like Yb : YAG, which need high pump power densities to overcome transparency threshold and efficient cooling at the same time. Because of an additionally high Stokes efficiency and good thermomechanical properties of the laser host, Yb : YAG was chosen as presently the most promising laser material to scale output power of the thin disc laser up to the kilowatt range.

For its promising properties, several groups have investigated Yb : YAG in the last ten years. After the first realization of a diode-pumped Yb : YAG laser by Fan at Lincoln Laboratory in 1990 [2], the operation at high output power was studied especially at Lawrence Livermore National Laboratory (LLNL), Hughes Research Laboratories (HRL), and Institut für Strahl-werkzeuge (IFSW) in collaboration with Deutsche Forschungszentrum für Luft- und Raumfahrt (DLR). At LLNL and HRL, the geometry of the laser active medium was a thin rod, which like the thin disc has a high ratio of cooling surface to active volume, but it exhibits strong thermal lensing. At HRL the Yb : YAG rod was side pumped, which allows a high transfer efficiency from the diode lasers to the rod, without any beam shaping. This has led to an early demonstration of high-power operation but with low optical efficiency and low beam quality; their highest published output power is 1040 W with approximately 22% optical efficiency [3]. At LLNL, the rod was end-pumped by a diode laser array using a lens duct with the highest output power of 1080 W using two rods [4]. At IFSW and DLR, the thin disc laser has been developed [1].

II. Numerical Studies

In order to determine the design and operation parameters of a thin disc laser that is expected to work at higher temperature, a numerical model is used. In particular, it allows the determination of the scaling properties of this laser concept. For the calculation various properties of Yb : YAG are needed, which are

Manuscript received December 15, 1999; revised April 24, 2000. This work was supported in part by the BMB+F under Contracts 13N6364, 13N6365, and 13N7300.

C. Stewen, M. Larionov, A. Giesen, and H. Hügel are with the Institut für Strahl-werkzeuge, Universität Stuttgart, Germany (e-mail: giesen@ifsw.uni-stuttgart.de).

K. Contag is with the Forschungsgesellschaft für Strahl-werkzeuge mbH, Stuttgart, Germany.

Publisher Item Identifier S 1077-260X(00)07080-5

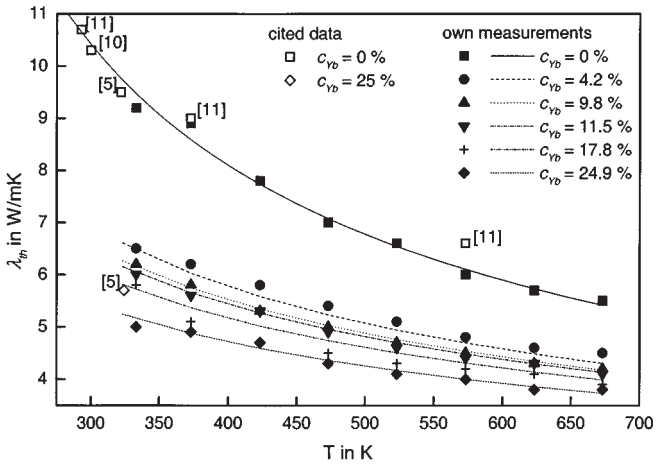

Fig. 2. Measured temperature dependence of the heat conductivity. Open symbols show literature data.

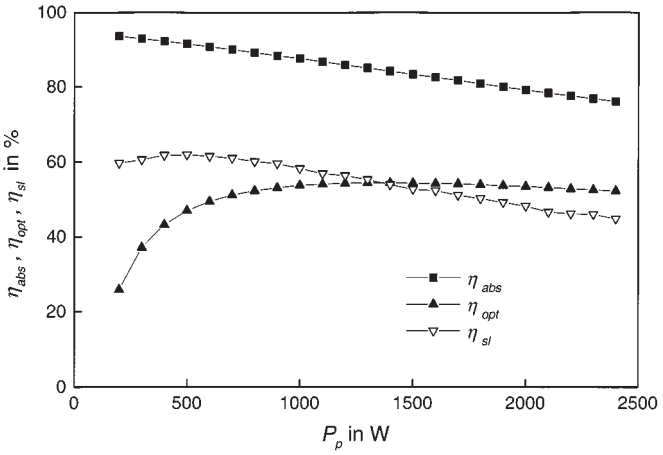

Fig. 3. Calculated dependence of absorption efficiency η_{abs}, optical efficiency η_{opt}, and slope efficiency η_{sl} on pump power P_p.

discussed in detail in [5], and all the material parameters used are summarized in [6]. As the temperature distribution inside the crystal has a strong effect on the output power, a detailed knowledge of the heat conductivity is important. Therefore, the temperature dependence of the heat conductivity has been measured within the frame of a subcontract (Austrian Research Centers Seibersdorf), as shown in Fig. 2. Based on these data, the following function represents the dependence of the heat conductivity λ_{th} on the doping concentration c_{Yb} and the temperature T

$$\lambda_{\mathrm{th}}(T, c_{\mathrm{Yb}}) = \lambda_{\mathrm{th}}(300\ \mathrm{K}, c_{\mathrm{Yb}}) \cdot \left(\frac{204\ \mathrm{K}}{T - 96\ \mathrm{K}}\right)^{0.48 - 0.46 * c_{\mathrm{Yb}}} \tag{1}$$

with the value of λ_{th} at 300 K

$$\lambda_{\mathrm{th}}(300\ \mathrm{K}, c_{\mathrm{Yb}}) = (7.28 - 7.3 * c_{\mathrm{Yb}})\ \mathrm{W/mK}. \tag{2}$$

For undoped YAG, the heat conductivity is given by

$$\lambda_{\mathrm{th}}(T) = \left[10.41 \cdot \left(\frac{204\ \mathrm{K}}{T - 96\ \mathrm{K}}\right)^{0.63}\right] \frac{\mathrm{W}}{\mathrm{mK}}. \tag{3}$$

The numerical model consists of three main steps: the calculation of the distribution of the absorbed pump radiation inside the crystal by Monte Carlo ray-tracing of the pump photons through the optical system, the calculation of the temperature distribution inside the crystal, and the calculation of the temperature-dependent output power. These three steps are repeated iteratively until a steady state is reached. The numerical code is discussed in more detail in [6] and [8] and has been verified by comparison with experimental results at low pump power using eight [6] and 16 absorption passes [9].

The generation of heat is assumed to result from two mechanisms: the Stokes defect of 8.6% between the energy of the pump and the laser photon on the one hand and the absorption of pump and laser radiation as well as fluorescence by the HR-coating of the crystal on the other hand. The heat load is calculated and the cooling medium is included, which is determined from finite-element calculations taking into account all mechanisms of heat transfer from the crystal to the cooling medium.

Based on former experiments and calculations, typical parameters of the thin disc laser for high-power operation are:

1) laser active medium:
   a) crystal thickness: $d = 200\ \mu$m;
   b) doping concentration: $c_{\mathrm{Yb}} = 8\%$;
   c) fraction of heat generation inside HR-coating: $f_{\mathrm{HR}} = 6\%$.
2) cooling:
   a) temperature of cooling medium: $T_c = 15\,^{\circ}$C;
   b) heat resistance: $R_{\mathrm{th}} = 12.7\ \mathrm{Kmm^2/W}$;
3) resonator:
   a) number of resonator passes through the crystal: $N_r = 2$;
   b) resonator internal losses: $L = 0.2\%$;
4) pump configuration and pump source:
   a) number of pump beam passes through the crystal: $N_p = 16$;
   b) pump power: $P_p = 1000$ W;
   c) central wavelength of pump radiation: $\lambda_c = 941.3$ nm;
   d) full-width half-maximum of pump radiation: $\Delta\lambda_H = 2$ nm;
   e) numerical aperture of the pump source: NA $= 0.15$;
   f) diameter of homogenizing pump source: $d_s = 5$ mm;
   g) ratio of pump source to pump spot diameter: 1 : 1.15.

A. Basic Dependences

Using these values and neglecting losses in the pump configuration and also not taking into account mechanical fracture limits, optical efficiencies as shown in Fig. 3 are calculated for varying pump power (the symbols inside this and all the other figures of this chapter represent discrete calculated data). Op-

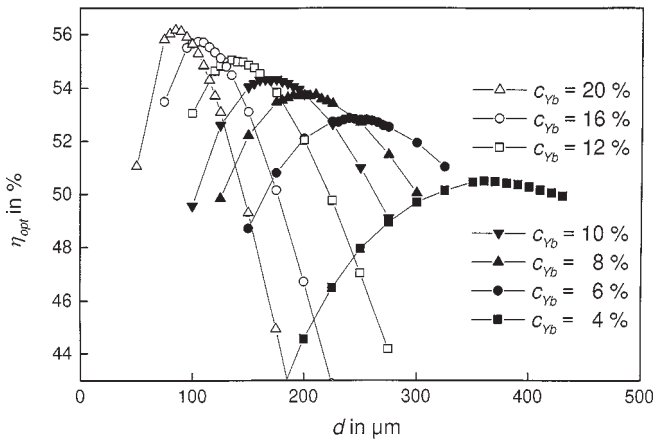

Fig. 4. Calculated optical efficiency as a function of crystal thickness at a pump power of 1000 W for different doping concentrations.

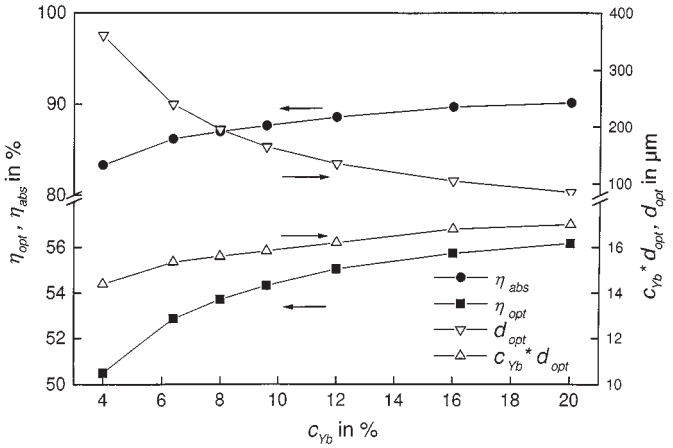

Fig. 5. Calculated dependence of optical efficiency $\eta_{\rm opt}$, absorption efficiency $\eta_{\rm abs}$, optimized crystal thickness $d_{\rm opt}$, and absorption length $c_{\rm Yb}d$ on doping concentration $c_{\rm Yb}$.

1000 W pump power, the output power is 540 W with 88% absorption efficiency, 58% slope efficiency, and a maximum temperature of the crystal at the front side of 130 °C. With higher pump power, the absorption efficiency is reduced due to higher temperature (11.5 °C per 100 W of pump power) and ground state depletion. This leads to a maximum optical efficiency of 54% at 1400 W pump power and a slight decrease of the optical efficiency.

The optical efficiency can be raised by reducing the crystal temperature, either by lowering the temperature of the cooling medium or by reducing the heat resistance between crystal and cooling fluid. At a pump power of 1000 W, the reduction of the heat resistance from 12.7 to 10 Km·m^2/W leads to an increase of optical efficiency from 54% to 56%, and the lowering of the temperature of the cooling medium from 15 °C to −50 °C yields an increase of the optical efficiency from 54% to 65%.

The dependence of the optical efficiency on the doping concentration and the crystal thickness at a pump power of 1000 W and for 16 absorption passes is shown in Fig. 4. By increasing the crystal thickness, the absorption efficiency and, therefore, the slope efficiency increases while the number of laser ions, which have to be pumped to transparency, also goes up and therefore the laser threshold increases. This means that an optimum crystal thickness exists for the highest optical efficiency.

The optimum crystal thickness decreases while the absorbing length $c_{\rm Yb} \cdot d$ increases with doping concentration, as shown in Fig. 5. Therefore, the absorption efficiency and the optical efficiency increase with increasing doping concentration. Changing the doping concentration from 4% to 20% increases the optical efficiency at 1000 W pump power from 50.5% to 56.2%. With higher doping concentration, however, a growing density of impurity ions may occur leading to a reduced fluorescence lifetime and an increased heat generation. These effects may compensate the increase in optical efficiency with increasing doping concentration. A decrease in fluorescence lifetime from 951 to, e.g., 800 μs would decrease the optical efficiency from 53.7% to 50.4%, and an increase in heat generation from 8.6% to 10% would decrease the optical efficiency to 51.2% using a doping

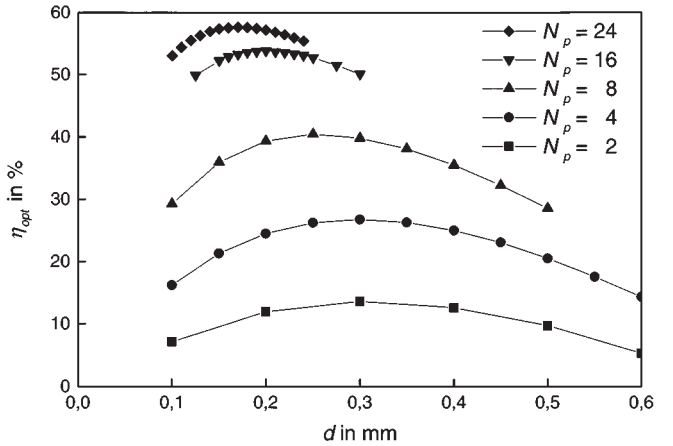

Fig. 6. Calculated optical efficiency $\eta_{\rm opt}$ versus crystal thickness d for different numbers of pump beam passes M_p at 1000 W pump power.

Optical efficiencies of more than 50% can be achieved by using 16 pump beam passes. Fig. 6 shows how the efficiency is influenced by the number of pump beam passes and the crystal thickness. With an increase from $N_p = 8$ to $N_p = 16$, the optical efficiency increases from 40% to 54%. Fig. 7 shows that the gain of optical efficiency is caused by the increased absorption efficiency due to a larger absorbing length, although the crystal thickness is reduced. Due to the higher absorption, the slope efficiency is higher and simultaneously the reduced crystal thickness leads to a lower laser threshold. Both aspects contribute to a rise of the optical efficiency.

B. Scaling of the Output Power

Scaling of the output power up to multi-kilowatt power levels is realized by scaling the pumped area at constant pump power density. This can be done either by enlarging the pump spot radius using one disc or by increasing the number of discs at constant pump spot radius.

Fig. 8 shows the dependence of the optical efficiency on pump

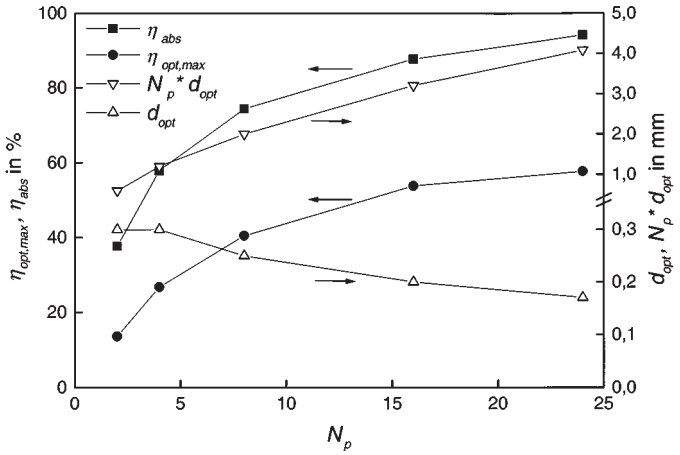

Fig. 7. Calculated dependence of the optimized optical efficiency $\eta_{\mathrm{opt,max}}$ and absorption efficiency η_{abs} as well as the optimized crystal thickness d_{opt} and the absorption length $d_{\mathrm{opt}} N_p$ on the number of pump beam passes N_p.

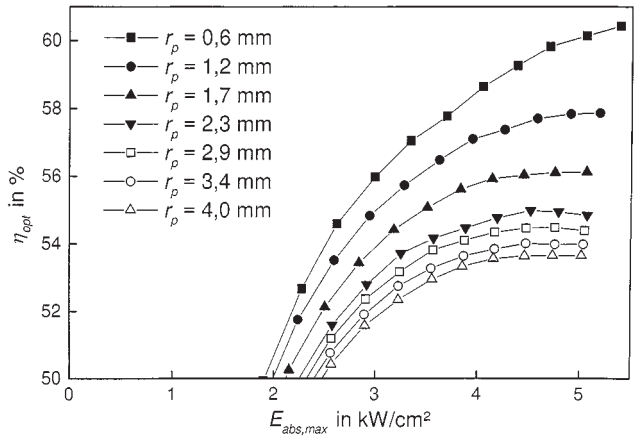

Fig. 8. Calculated dependence of optical efficiency η_{opt} on the absorbed pump power density $E_{\mathrm{abs,max}}$ for different pump spot radii.

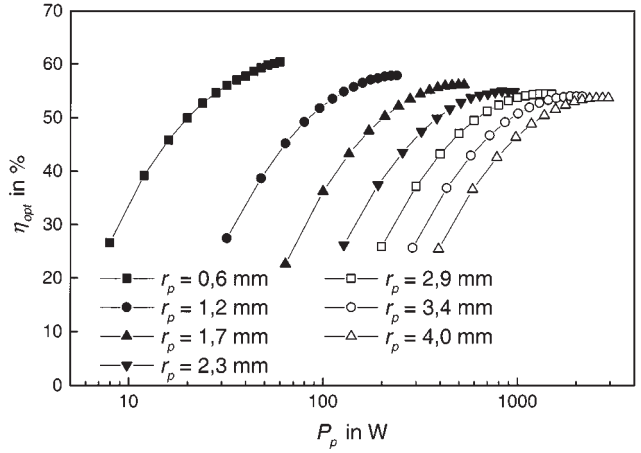

Fig. 9. Calculated dependence of optical efficiency η_{opt} on pump power P_p for different pump spot radii r_p.

show a slight decrease in optical efficiency with increased pump spot diameter. This is due to the radial heat flux inside the crystal

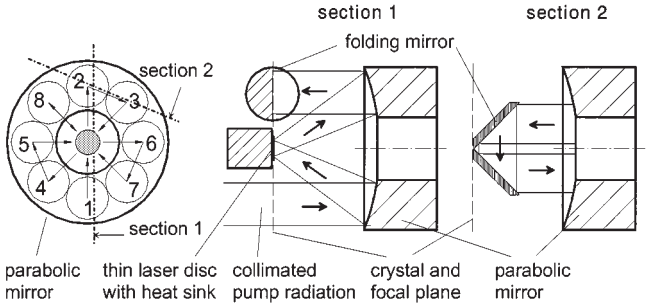

Fig. 10. Principal setup of the pump geometry allowing 16 absorption passes using a parabolic mirror.

crystal temperature (in the calculations this is included as an increased effective heat resistance). As a consequence, the absorption efficiency and hence the optical efficiency will be lower.

The other possibility of enlarging the pumped area is an increased number of discs. The numerical model shows that the optical efficiency remains constant, although the resonator internal losses increase proportional to the number of discs.

III. Experimental Setup

Two modules of stacked arrays, which are the first realizations of such modules, built in 1997, one from Jenoptik Laserdiode GmbH and one from Dilas Diodenlaser GmbH, are used as pump sources for scaling the laser output power up to 1 kW. The electric-optical efficiencies of these modules, defined as the ratio between the output power with the specified beam parameter product of 750 mm·mrad and the consumed electric power of the diodes, are 22.5% and 29.3%, respectively. To homogenize the radiation of the stacked arrays, it is coupled into a silica rod with 5 mm diameter, 200 mm length, and a numerical aperture of NA $\leq$ 0.15. The fraction of pump radiation lost in the homogenizing rod is 6%. The realization of 16 absorption passes of the pump radiation has been done by two different pump configurations.

The configuration using a parabolic mirror [9] for pumping one crystal is shown in Fig. 10. The collimated pump radiation hits segment 1 of the parabolic mirror and is focused onto the crystal, which is placed in the focal plane (this is shown in Section 1 of Fig. 10). The unabsorbed pump radiation is collimated again when it hits segment 2 of the parabolic mirror. Reflected by two folding mirrors, the radiation hits the parabolic mirror on segment 3 (shown in Section 2 of Fig. 10). Then the radiation is imaged onto the crystal again. Using two additional pairs of folding mirrors and the other segments of the parabolic mirror, eight absorption passes through the crystal are achieved. A final flat reflector reverses the path of the pump radiation, generating 16 absorption passes. The device, which has been used in the experiments, is shown in Fig. 11. With this device the scaling of the output power by increasing the diameter of the pump spot has been realized.

For the investigation of the scaling of output power using several discs, a configuration as shown in Fig. 12 is used. It integrates four crystals and two pump sources. The crystal and

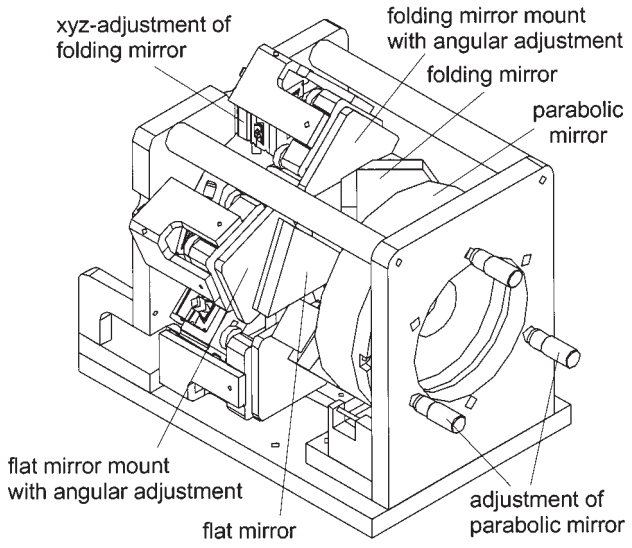

Fig. 11. Experimental pump configuration for one crystal.

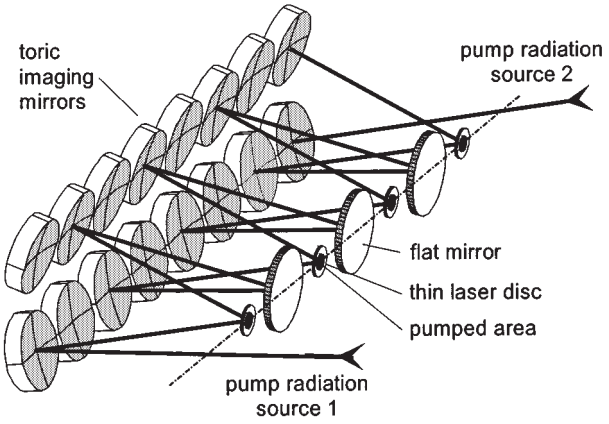

Fig. 12. Principal setup of the pump geometry for four crystals using two pump sources allowing 16 absorption passes.

this as a center line. In Fig. 12, the propagation of the radiation from pump source 1 through all the mirrors and pumped discs is shown. The collimated radiation is focused onto the first crystal by using a toric mirror. The unabsorbed radiation is collimated by another toric mirror, reflected by a flat mirror, and then hits the next toric mirror. Using collimating mirrors in an optical distance of two times the focal length between two successive elements, the divergence of the pump radiation can be kept constant. Following the path of the radiation up to the final mirror, which is spherical, each crystal is pumped by two absorption passes. The final mirror reverses the path of the pump radiation again to generate another two absorption passes through each crystal, which gives a total of 16 absorption passes for the pump radiation. The pump configuration that has been realized for the experiments is shown in Fig. 13.

IV. Experiments

A. Scaling of Output Power Using One Disc

With one disc, scaling of the output power is investigated by

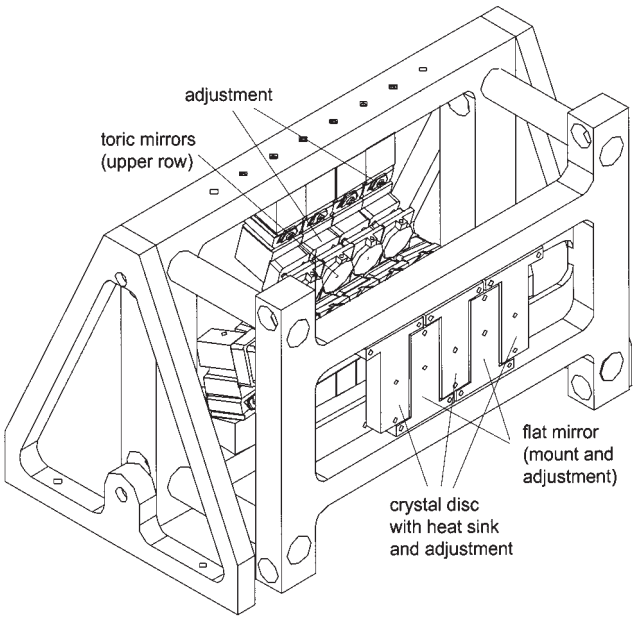

Fig. 13. Experimental pump configuration for up to four crystals.

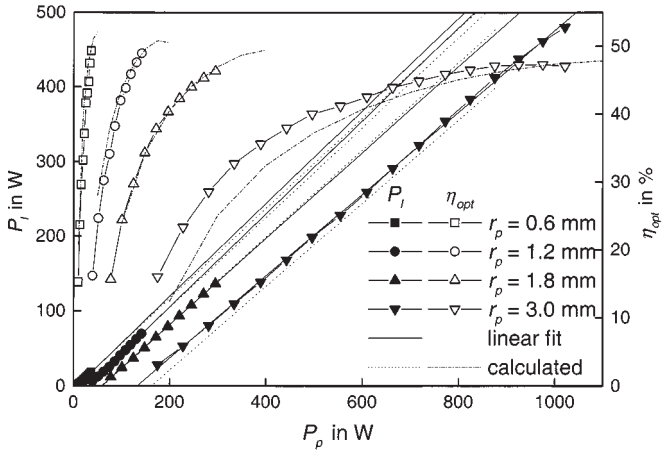

Fig. 14. Laser output power P_l and optical efficiency $\eta_{\rm opt}$ in comparison of experimental and calculated results for various radii r_p of the pump spot.

radius of the pump spot can be varied. Fig. 14 shows the experimental results obtained with four different pump spot sizes in comparison to numerical results. In these calculations, the measured losses of the optics of the pump configuration are taken into account, in contrast to the results reported in Section II. The resonator consists of the laser crystal as end mirror and an outcoupling mirror with 1 m radius of curvature and 2.2% transmission; its length is 40 cm. The thickness of the crystal was 230 μm, and the doping concentration 8%. The highest output power was 480 W with 47% optical efficiency with respect to the incident pump power. With the smallest pump spot, the optical efficiency was 49%. This slightly decreased efficiency with larger pump spots reflects the reduced contribution to cooling of the radial heat flux within the crystal. This results in a higher crystal temperature, which leads to a reduced absorption efficiency and an increased threshold and therefore to a reduced

DOCKET ALARM

Explore Litigation Insights

Docket Alarm provides insights to develop a more informed litigation strategy and the peace of mind of knowing you're on top of things.

Real-Time Litigation Alerts

Keep your litigation team up-to-date with **real-time alerts** and advanced team management tools built for the enterprise, all while greatly reducing PACER spend.

Our comprehensive service means we can handle Federal, State, and Administrative courts across the country.

Advanced Docket Research

With over 230 million records, Docket Alarm's cloud-native docket research platform finds what other services can't. Coverage includes Federal, State, plus PTAB, TTAB, ITC and NLRB decisions, all in one place.

Identify arguments that have been successful in the past with full text, pinpoint searching. Link to case law cited within any court document via Fastcase.

Analytics At Your Fingertips

Learn what happened the last time a particular judge, opposing counsel or company faced cases similar to yours.

Advanced out-of-the-box PTAB and TTAB analytics are always at your fingertips.

API

Docket Alarm offers a powerful API (application programming interface) to developers that want to integrate case filings into their apps.

LAW FIRMS
Build custom dashboards for your attorneys and clients with live data direct from the court.

Automate many repetitive legal tasks like conflict checks, document management, and marketing.

FINANCIAL INSTITUTIONS
Litigation and bankruptcy checks for companies and debtors.

E-DISCOVERY AND LEGAL VENDORS
Sync your system to PACER to automate legal marketing.